

Titanium Surfaces Functionalized with siMIR31HG Promote Osteogenic Differentiation of Bone Marrow Mesenchymal Stem Cells

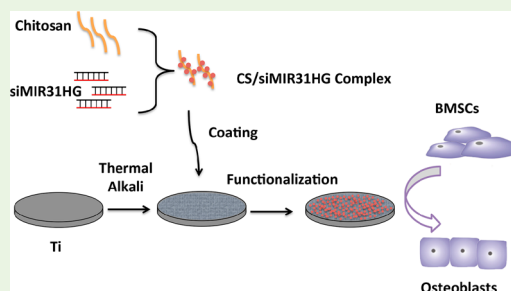
Yiping Huang,^{†,‡} Yunfei Zheng,^{†,‡} Yongxiang Xu,[§] Xiaobei Li,[‡] Yan Zheng,[⊥] Lingfei Jia,^{*,||} and Weiran Li^{*,‡,#}

[†]Department of Orthodontics, [§]Department of Dental Materials, [⊥]Department of Oral Implantology, and ^{||}Central Laboratory, Peking University School and Hospital of Stomatology, Beijing 100081, China

[#]National Engineering Laboratory for Digital and Material Technology of Stomatology, Beijing Key Laboratory of Digital Stomatology, Beijing 100081, China

ABSTRACT: Titanium (Ti) implants are widely used in the clinic as bone substitutes and dental implants, but further improvements are needed to obtain high osteogenic ability and consequent osseointegration. Knockdown of long noncoding RNA MIR31HG promotes osteogenic differentiation and bone formation. In this study, we fabricated a Ti surface functionalized with siRNA targeting MIR31HG (siMIR31HG) and accelerated osteogenesis of bone marrow mesenchymal stem cells (BMSCs). Chitosan/siRNA complex was loaded onto the thermal alkali-treated Ti surface to fabricate the siMIR31HG-functionalized Ti surface. The surface morphology, siRNA loading and release efficiency, and transfection efficacy were investigated, and the biological effects, such as cell proliferation, cell morphology, and osteogenic activity, were determined. The results showed that the siMIR31HG-functionalized Ti implant generated an ~50% knockdown of MIR31HG, with no apparent cytotoxicity, which consequently enhanced osteogenic differentiation of BMSCs, as indicated by the increase of ALP production, extracellular matrix mineralization, osteogenic gene expression, and ectopic bone formation in vivo. The siMIR31HG biofunctionalization can be used to obtain better osseointegration of Ti implant in the clinic.

KEYWORDS: titanium, surface functionalization, siMIR31HG, osteogenic differentiation, bone marrow mesenchymal stem cells



INTRODUCTION

Titanium (Ti) implants are widely used as bone substitutes and dental implants because of their excellent biocompatibility, mechanical property, and osseointegration capacity.^{1,2} However, the deficient bioactivity and slow osseointegration of these materials still lead to implant failure. Surface modification of Ti implants is an effective method to enhance bioactivity for better osseointegration.³ Biomolecules, such as extracellular matrix (ECM) components,⁴ growth factors,⁵ and peptides,⁶ have been loaded onto biomaterials. However, this biofunctionalization does not directly target the molecular mechanism and thereby generates limited biological effects. Biofunctionalization using nucleic acids to affect key molecules in osteogenesis may effectively improve the osseointegration of Ti implants.

Noncoding RNAs (ncRNAs) serve as important regulatory mediators in biological and pathological control,⁷ and some small ncRNAs has been demonstrated to regulate osteogenesis. Previous studies have used miRNAs, including miR-21,⁸ miR-26a,⁹ miR-29b,¹⁰ and miR-148b,¹¹ in biofunctionalization of biomaterials. In contrast, long noncoding RNAs (lncRNAs), defined as ncRNAs > 200 nt in length, have not been applied in the modification of Ti surfaces. lncRNAs can regulate a

panel of genes simultaneously and also serve as a miRNA sponge to target downstream molecules. They possess the ability to induce the commitment of mesenchymal stem cells (MSCs) into bone tissue effectively,^{12,13} indicating a potential approach for promotion of biomaterial osseointegration by manipulating lncRNA levels.

MIR31HG (also known as LOC554202), which is located on chromosome 9 (9p21.3),¹⁴ participates in a wide range of cell functions. We have found that knockdown of MIR31HG expression significantly promotes osteogenesis and bone formation.¹⁵ Thus, we chose MIR31HG as a knockdown target for Ti surface functionalization to enhance osteogenic activity. RNA interference by small interfering RNAs (siRNAs) is a valuable approach to silence the targeted gene, and certain reports exist on use of the siRNA delivery system to biofunctionalize tissue engineering scaffolds.^{16,17} Thus, we intend to apply siRNA targeting MIR31HG (siMIR31HG) to functionalize Ti implant and obtain better osteogenic activity.

Received: April 8, 2018

Accepted: June 14, 2018

Published: June 14, 2018

Table 1. Oligonucleotides Sequences

name	sense strand/sense primer (5'-3')	antisense strand/antisense primer (5'-3')
	primers for qRT-PCR	
MIR31HG	TCTCTGGTGCTTCCCTCCTT	GATCTAAGCTTGAGCCCCCA
ALP	ATGGGATGGGTGTCTCCACA	CCACGAAGGGGAAGTGTCT
RUNX2	CCGCTCAGTGATTTAGGGC	GGGTCTGTAATCTGACTCTGTCC
OCN	CACTCCTCGCCCTATTGGC	CCCTCCTGCTTGACACAAAG
GAPDH	GGTCACCAGGGCTGCTTTTA	GGATCTCGCTCCTGGAAGATG
	siRNAs	
siNC	UUCUCCGAACGUGUCACGUTT	ACGUGACACGUUCGGAGAATT
siMIR31HG	GGAGCGCUUUGUGUGAGAAGUUGAA	UUCAACUUCACACAAAGCGCUCC

In the siRNA-functionalized coating technique, the loading capacity of the Ti surface, siRNAs loading and delivery strategy must all be considered. The pure Ti implant surfaces have rather limited loading capacity, and the porous structure generated by thermal alkali treatment on the Ti surface is a promising method for increasing its reservoir capacity.^{18–20} For siRNAs loading and delivery strategy, chitosan (CS) constitutes a good vector candidate due to its good biocompatibility, natural biodegradability, and oligonucleotides delivery efficiency. It has been reported to carry abundant siRNA with good cytocompatibility.^{19,21,22} Thus, we used a siMIR31HG-biofunctionalized coating method on a Ti surface by loading the CS/siMIR31HG complex onto a thermal alkali-treated Ti surface. The surface morphology, siRNA localization, gene knockdown ability, and cytotoxicity were determined, and the efficacy in promoting osteoblastic differentiation of bone marrow mesenchymal stem cells (BMSCs) was investigated in vitro and in vivo. This study is expected to advance the use of Ti implants with enhanced osseointegration.

MATERIALS AND METHODS

RNA Oligoribonucleotide. Chemically modified siMIR31HG labeled or not labeled with Cy3 and negative control siRNA (siNC) labeled or not labeled with Cy3 were obtained from GenePharma Co. (Shanghai, China). The oligoribonucleotide sequences are listed in Table 1.

Preparation of the siRNA-Functionalized Titanium Surface. Commercially pure Ti discs were supplied by Wego Jericom Biomaterials Co. (Weihai, China). The dimension of Ti discs used for the in vitro experiments were Φ 33 \times 1.5 mm and Φ 15 \times 1 mm, and the dimension was Φ 5 \times 1.5 mm for the in vivo experiments. The Ti discs were treated using the thermal alkali process. The pure Ti discs were immersed in 5 M NaOH solution at 60 °C for a day. After ultrasonic cleaning with deionized water and drying in air, the samples were sterilized for 30 min. The chitosan (CS)/siRNA functionalized surface was formed as previously described.¹⁹ In brief, chitosan was diluted in sodium acetate buffer (1 mg/mL solution, pH 5.5). After that, 20 μ L amounts of siRNA (100 μ M) were mixed with 1 mL chitosan solution, followed by stirring, and allowed to react for 1 h. The thermal alkali-treated Ti discs were soaked in the CS/siRNA solution at 4 °C for a day. Subsequently, the Ti discs were washed with acetate buffer and dried to obtain the siRNA-functionalized Ti surfaces.

siRNA Loading Profile. The siRNA labeled with Cy3 was used to determine its loading efficiency as described previously.²³ After soaking Ti samples in the CS/siRNA solution for 2, 4, 8, 12, and 24 h, we obtained 10 μ L amounts of the supernatant to determine the residual siRNA by a FLUOstar plate reader (BMG LABTECH, Ortenberg, Germany). The loading efficiency was calculated by subtracting the remaining siRNA amount from the initial amount.

Surface Characterization. The surface morphology of Ti samples was scanned by scanning electron microscopy (SEM, Hitachi

S-4800, Tokyo, Japan). The functionalized surface of siRNAs labeled with Cy3 was scanned via confocal laser scanning microscopy (Carl Zeiss, Jena, Germany). Energy-dispersive X-ray (EDX) microanalysis of the Ti samples was performed using SEM and TEAM EDS Software (EDAX Inc., Mahwah, New Jersey, USA). The EDX spectra were collected from the specimens, and elemental analysis (weight% and atomic%) was performed. Static contact angles were determined using a SL200 contact angle system (Kino Industry, New York, NY, USA). We captured images of the water droplet on Ti surfaces and measured the contact angle.

Cumulative siRNA Release Profile. Cumulative siRNA release efficiency was determined as described previously.²³ The siRNA labeled with Cy3 was functionalized on the Ti samples. Then, the Ti discs was soaked in the phosphate buffered saline (PBS). At the scheduled time, we collected the supernatant and replaced with fresh PBS. After all supernatant obtained, the siRNA amount was determined by fluorescence intensity measurement. The cumulative siRNA release was measured by adding all the siRNA amounts from previous time points.

Cell Culture and Osteogenic Induction. Primary BMSC lines were obtained from ScienCell (San Diego, CA, USA) and cultured in α -minimum essential medium (Gibco, Grand Island, NY, USA) supplemented with 10% fetal bovine serum (Gibco) and 1% penicillin/streptomycin (Invitrogen, Carlsbad, CA, USA). Osteogenic differentiation of BMSCs was induced using osteogenic medium containing 10 mM β -glycerophosphate (Sigma-Aldrich, Saint Louis, MO, USA), 200 μ M L-ascorbic acid (Sigma-Aldrich), and 100 nM dexamethasone (Sigma-Aldrich).

Cell Transfection. Transient transfection of siRNAs into BMSCs was performed using Lipofectamine 3000 (Invitrogen) according to the manufacturer's procedure. Cells in 6-well plates were transfected with siRNAs at 100 nM. The cells were harvested 24 h after transient transfection.

For transfection of the siRNAs on the Ti samples, the cells were inoculated on the samples, and at the indicated time points, the cells were harvested.

Cell Viability. The cell viability assay was performed using the Cell Counting Kit-8 (CCK-8, Dojindo, Kumamoto, Japan) according to the manufacturer's instructions.²⁴ Briefly, BMSCs were seeded onto different Ti surfaces. At the scheduled time, CCK-8 reagent was added into each well and further incubated for 3 h. Subsequently, the supernatant was collected into a 96-well plate, and the absorbance was measured at 450 nm using a spectrophotometer (BioTek Instruments Inc., Winooski, VT, USA).

Cell Morphology. The BMSCs were seeded on different Ti samples in 24-well plates. After 24 h of culture, the cells were rinsed with PBS, fixed with 2.5% glutaraldehyde, dehydrated with a graded ethanol series at 4 °C, and finally freeze-dried. The cell morphology was characterized using SEM.

Alkaline Phosphatase (ALP) Staining and Activity. The BMSCs were seeded onto different Ti samples placed in 24-well plates. After 24 h of incubation, the medium was changed to osteogenic induction medium. After culturing for 7 days, ALP staining and activity were performed, as described previously.^{15,25} ALP staining was performed according to the NBT/BCIP staining kit protocol (CoWin Biotech, Beijing, China). In brief, the cultured cells

were washed with PBS and fixed with 4% paraformaldehyde. The cell layer was then incubated in an alkaline solution at 37 °C in the dark for 20 min.

ALP activity was performed using a colorimetric assay kit (Biovision, Milpitas, CA, USA). The cells were washed with PBS, permeabilized with 1% Triton X-100, scraped into distilled water, and subjected to three cycles of freezing and thawing. ALP activity was determined at 405 nm using p-nitrophenyl phosphate as a substrate. Total protein content was measured by the bicinchoninic acid method of the Pierce protein assay kit (Thermo Fisher Scientific, Rockford, IL, USA). ALP activities relative to that of the control were calculated after normalization to the protein content.

Alizarin Red S Staining and Quantification. The cells were cultured in a similar manner as in ALP staining assay. At day 14 of osteogenic culturing, mineralization was detected by Alizarin red S staining, as previously described.^{15,25} The cells were fixed with 4% paraformaldehyde and stained with 0.1% Alizarin red S (pH 4.2, Sigma-Aldrich). For quantitative assessment, the stain was eluted with 100 mM cetylpyridinium chloride (Sigma-Aldrich) and quantified by spectrophotometric absorbance at 570 nm. Alizarin red S intensity relative to that of the control was calculated after normalization to the protein content.

RNA Isolation and Quantitative Reverse Transcription (qRT-PCR). The RNA was extracted using TRIzol reagent (Invitrogen) according to the manufacturer's procedure and reverse-transcribed into cDNA using a Reverse Transcription kit (Takara, Tokyo, Japan). qRT-PCR was performed on 1 μ g amounts of total RNA using the SYBR Green Master Mix on an ABI Prism 7500 real-time PCR System (Applied Biosystems, Foster City, CA, USA). The following thermal settings were used: 95 °C for 10 min followed by 40 cycles of 95 °C for 15 s and 60 °C for 1 min. The primers used for MIR31HG, ALP, RUNX2, osteocalcin (OCN), and glyceraldehyde 3-phosphate dehydrogenase (GAPDH, internal control) are listed in Table 1. The data were calculated using the $2^{-\Delta\Delta Ct}$ relative expression method as previously described.^{15,25}

Immunofluorescence Staining. Immunofluorescence staining was performed as described previously.^{15,25} Cells grown on the Ti surfaces after 7 days of osteogenic induction were fixed with 4% paraformaldehyde, permeabilized with 0.1% Triton X-100, and blocked with 3% bovine serum albumin (Sigma-Aldrich). After that, the cells were incubated with 1:200 primary antibody against OCN (Abcam, Cambridge, UK) or RUNX2 (Cell Signaling Technology, Beverly, MA, USA) at 4 °C overnight and next day incubated with 1:500 specified secondary antibodies (Cell Signaling Technology) for 1 h. Nuclei were counterstained with DAPI, and the Ti samples were mounted on a glass slide. Images were captured with a confocal imaging system (Carl Zeiss).

Ectopic Bone Formation in Vivo. Ti samples coated with BMSCs after 7 days of osteogenic induction were implanted subcutaneously on the back of 6-week-old male BALB/c homozygous nude (nu/nu) mice (10 mice per group), according to previous study design.^{15,25} After 8 and 12 weeks, the implants were harvested, fixed with formalin, and infiltrated by resin. The hard tissue slices were generated and stained with hematoxylin and eosin (H&E).

Statistical Analysis. Statistical analyses were conducted using SPSS software (IBM, Armonk, NY, USA). Data are presented as the mean \pm SD of the values from at least three independent experiments. Differences between groups were measured using Student's *t*-test. In cases of multiple-group testing, one-way analysis of variance and Student–Newman–Keuls posthoc test were conducted. A *P*-value <0.05 was considered statistically significant.

RESULTS

Characterization of the siRNA-Functionalized Titanium Surface. To achieve siRNA-functionalized titanium surface, the siRNA loading efficiency was determined first. After 8 h of soaking, the siRNA loading efficiency was nearly 70% (Figure 1A). The cumulative siRNA release profile from functionalized Ti surface was then monitored over 7 days. The

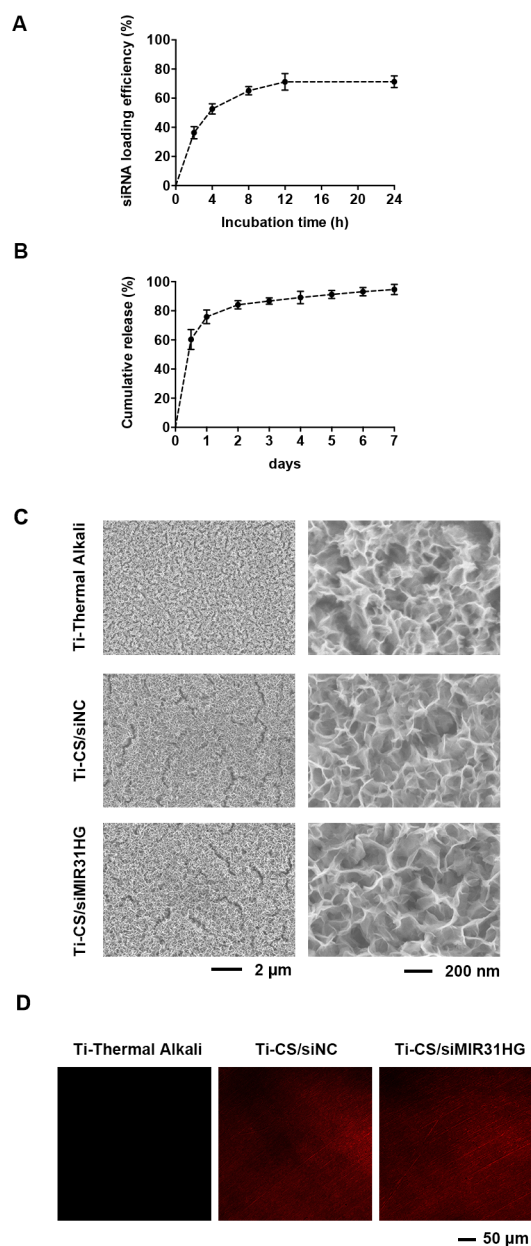


Figure 1. Morphology of different Ti samples. (A) siRNA loading efficiency on the thermal alkali-treated Ti surface. (B) Cumulative siRNA release profile from the siRNA-functionalized Ti surface. (C) SEM images showing the morphology of the thermal alkali-treated Ti surface (Ti-Thermal Alkali), siNC-functionalized Ti surface (Ti-CS/siNC), and siMIR31HG-functionalized Ti surface (Ti-CS/siMIR31HG). Scale bar, 2 μ m (left) and 200 nm (right). (D) Fluorescence confocal laser scanning microscope images of the thermal alkali-treated Ti surface, and Cy3-labeled siNC- and siMIR31HG-functionalized Ti surfaces. Scale bar, 50 μ m.

siRNA was released mostly (\sim 80%) within the first day, and then released slowly and steadily, and nearly reached 100% at day 7 (Figure 1B).

The morphologies of the Ti surfaces with or without siRNA functionalization were scanned using SEM. The Ti surface after thermal alkali treatment with or without siRNA functionalization both displayed a microporous structure with pore diameters ranging from 100 to 500 nm (Figure 1C). To determine the distribution of CS/siRNA on the surface, the siRNAs labeled with Cy3 were used and scanned by laser

scanning confocal microscopy. The fluorescence images demonstrated that the CS/siRNA particle was distributed uniformly on the functionalized Ti surface (Figure 1D).

In energy-dispersive X-ray microanalysis, Ti was the first main element and carbon was the second main element in the tested Ti discs according to weight percentage. Sodium element was detected on the Ti samples treated with thermal alkali. On the siRNA-functionalized Ti surfaces, the weight and atomic percentages of nitride element were greater than that of the thermal alkali-treated group. The mean atomic percentage of phosphorus element was significantly increased on the siMIR31HG-functionalized surface (Figure 2A).

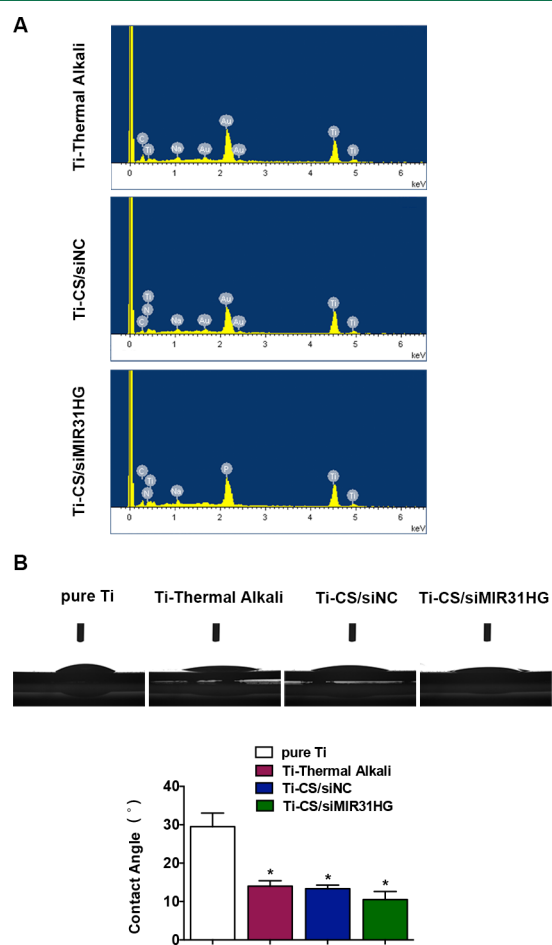


Figure 2. Characterization of Ti samples. (A) Energy-dispersive X-ray (EDX) microanalysis of the corresponding Ti surfaces. (B) Water contact angle (upper) and quantification (lower) of the pure Ti surface (pure Ti), thermal alkali-treated Ti surface (Ti-Thermal Alkali), siNC-functionalized Ti surface (Ti-CS/siNC), and siMIR31HG-functionalized Ti surface (Ti-CS/siMIR31HG). Data are showed as mean \pm SD (* $P < 0.05$).

The hydrophilicity of the Ti surfaces was evaluated using the water contact angle. The water contact angle for the pure Ti surface was $\sim 30^\circ$. The contact angle of the thermal alkali-treated surface and the siRNA-functionalized surface were all decreased, indicating better hydrophilicity than the pure Ti surface (Figure 2B).

Transfection Efficacy of the siRNA-Functionalized Titanium Surface. To evaluate the gene knockdown efficacy, we first transfected siRNAs into BMSCs. The MIR31HG expression was significantly downregulated by $\sim 60\%$ at 24 h

after transfection of siMIR31HG (Figure 3A). We then seeded BMSCs on the siRNA-functionalized surface. The cells were

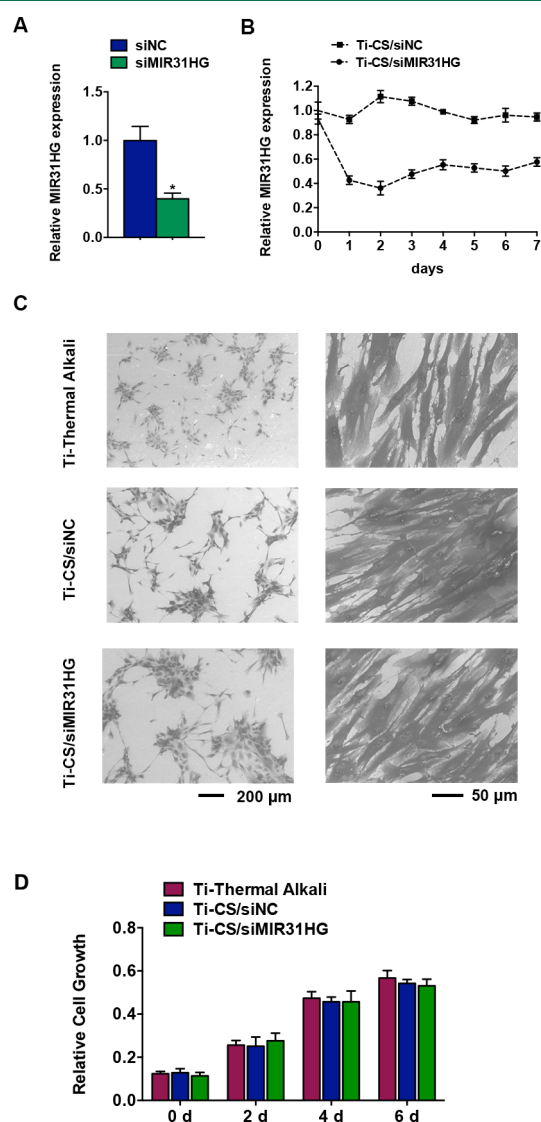


Figure 3. MIR31HG knockdown efficacy and biocompatibility of siRNA-functionalized Ti samples. (A) Relative MIR31HG expression determined by qRT-PCR in BMSCs transfected with siNC or siMIR31HG. (B) Relative MIR31HG expression in BMSCs after culture on the siNC-functionalized Ti surface (Ti-CS/siNC) and siMIR31HG-functionalized Ti surface (Ti-CS/siMIR31HG) at the indicated time. (C) SEM images showing the cell morphology 24 h after seeding on the corresponding Ti surfaces. Scale bar, 200 μm (left) and 50 μm (right). (D) Relative cell growth of BMSCs on the corresponding Ti surfaces determined by CCK-8 assay at 2, 4, and 6 days. Data are showed as mean \pm SD (* $P < 0.05$).

harvested and the RNA was extracted at the indicated time points. Compared with the siRNA control surface, the intracellular MIR31HG expression decreased by $\sim 60\%$ on the siMIR31HG-functionalized surface within the first day, and the MIR31HG expression remained at a low level and decreased by $\sim 40\%$ at day 7 (Figure 3B).

Cell Morphology and Viability. The cell morphology and viability were assessed after seeding and growth of BMSCs on the Ti surfaces. The cells showed similar morphology and spread well on the three Ti surfaces (Figure 3C). The CCK-8

assay showed that no significant difference of cell growth was found in the siRNA-functionalized group compared with the thermal alkali-treated surface (Figure 3D). No apparent difference of cell viability was found between the siMIR31HG-functionalized surface and the siRNA control surface (Figure 3D).

Osteogenic Capacity. The osteogenic capacity of BMSCs on the Ti samples was evaluated using ALP production, ECM mineralization, and osteogenic gene expression. At day 7 of osteoblastic induction, ALP staining and activities were similar on the thermal alkali-treated surface and the siRNA control surface, whereas the siMIR31HG-functionalized surface induced higher ALP production (Figure 4A). At day 14 of

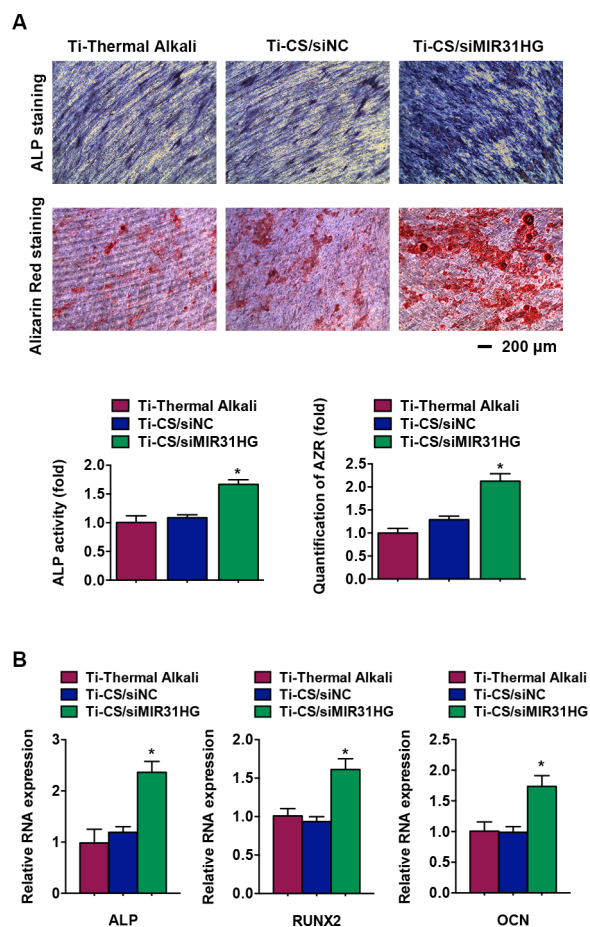


Figure 4. Osteogenic capacity of BMSCs on Ti samples. (A) ALP staining and ALP activity of BMSCs at day 7 of osteogenic induction on the thermal alkali-treated Ti surface (Ti-Thermal Alkali), siNC-functionalized Ti surface (Ti-CS/siNC), and siMIR31HG-functionalized Ti surface (Ti-CS/siMIR31HG). Alizarin red staining (AZR) and quantification of BMSCs at day 14 of osteogenic induction on the corresponding Ti surfaces. Scale bar, 200 μm . (B) Relative mRNA expression of ALP, RUNX2, and OCN at day 7 of osteogenic induction on the corresponding Ti surfaces. Results are shown as mean \pm SD (* P < 0.05).

osteoblastic induction, the ECM mineralization, as indicated by Alizarin red S staining, was significantly enhanced on the siMIR31HG-functionalized surface compared with the siRNA control surface as well as the thermal alkali-treated surface (Figure 4A). The osteogenic gene expression showed a similar trend. The mRNA expression of ALP, RUNX2, and OCN as determined by qRT-PCR was significantly increased on the

siMIR31HG-functionalized surface at day 7 of osteoblastic induction (Figure 4B). Immunofluorescence images also demonstrated that the intensity of immunostaining of OCN (Figure 5A) and RUNX2 (Figure 5B) was higher on the siMIR31HG-functionalized surface than the control groups at day 7 of osteoblastic differentiation.

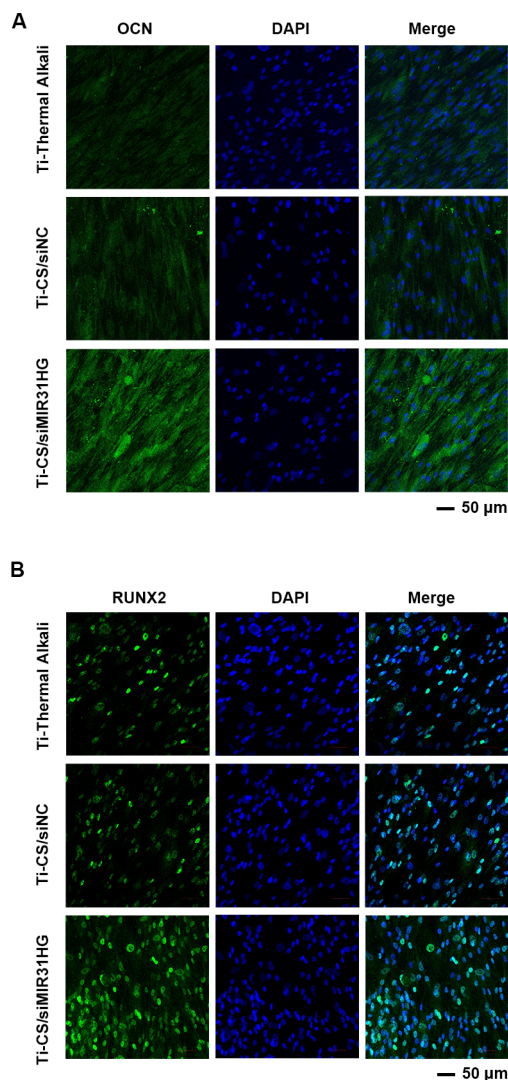


Figure 5. Confocal microscopy of (A) OCN and (B) RUNX2 with DAPI counterstaining of BMSCs at day 7 of osteogenic induction on the thermal alkali-treated Ti surface (Ti-Thermal Alkali), siNC-functionalized Ti surface (Ti-CS/siNC), and siMIR31HG-functionalized Ti surface (Ti-CS/siMIR31HG). Scale bar, 50 μm .

Ectopic Bone Formation. To further determine the osteogenic capacity, the ectopic bone formation assay was applied (Figure 6A). After 8 weeks of implantation, the new-bone layer as acidophilic tissue under H&E staining was formed on the surfaces of the Ti specimen. The bone matrix formation increased on the siMIR31HG-functionalized surface (Figure 6B). After 12 weeks of implantation, the bone matrix layer was also greater on the siMIR31HG functionalization group than the siRNA control group (Figure 6C).

DISCUSSION

Biofunctionalization of Ti surface to target specific molecules in osteogenesis is an effective approach to develop an implant

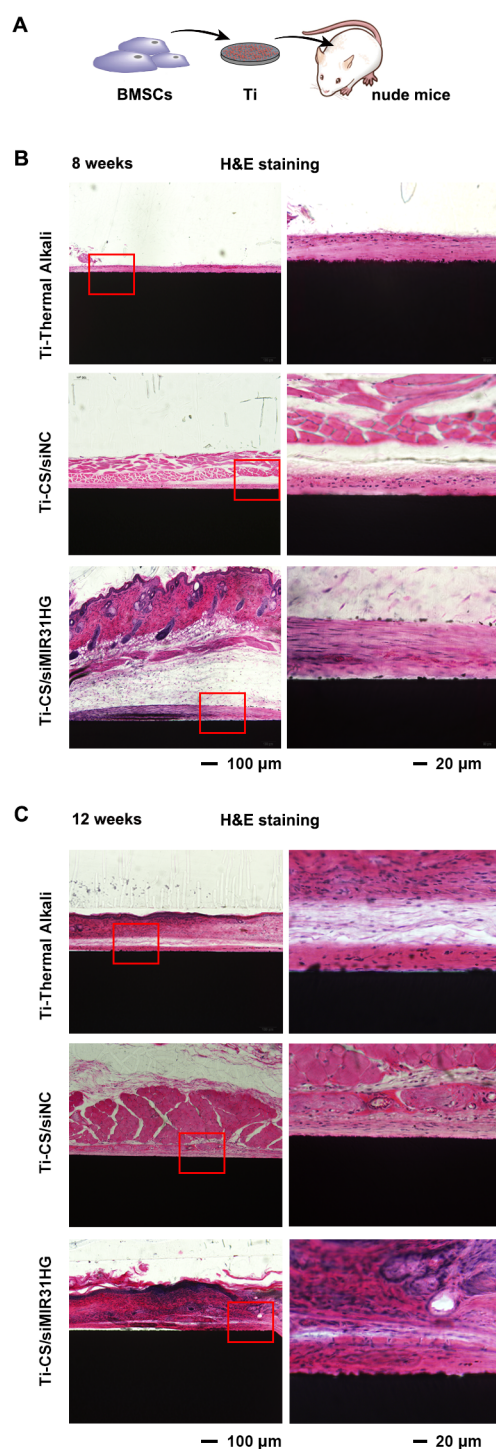


Figure 6. siMIR31HG-functionalized Ti surface promoted bone formation in vivo. (A) Schematics showing the experimental setup. (B) H&E staining of the thermal alkali-treated Ti samples (Ti-Thermal Alkali), siNC-functionalized Ti samples (Ti-CS/siNC), and siMIR31HG-functionalized Ti samples (Ti-CS/siMIR31HG) after 8 weeks of implantation. Scale bar, 100 μm (left) and 20 μm (right). (C) H&E staining of Ti-Thermal Alkali, Ti-CS/siNC, and Ti-CS/siMIR31HG samples after 12 weeks of implantation. Scale bar, 100 μm (left) and 20 μm (right).

with better osseointegration. In this study, the Ti surface was treated with thermal alkali and subsequently functionalized with the CS/siRNA particles. This coating technique displayed

good biocompatibility, siRNA loading and release efficiency, and gene knockdown efficacy. The siMIR31HG-functionalized titanium surface significantly improved the osteoblastic differentiation of BMSCs in vitro and in vivo.

The siMIR31HG biofunctionalization improved the osteogenic activity of Ti surface, as revealed by the increase of ALP activity, ECM mineralization, and osteogenic gene expression in vitro, and ectopic bone formation in vivo. Some studies have used biomolecules for biofunctionalization, including ECM components,⁴ growth factors,⁵ and peptides.⁶ However, this biofunctionalization does not target the molecules in osteogenesis directly, and peptides or proteins usually require high doses to function, resulting in a limited effect.³ Loading the biomaterial with a therapeutic oligonucleotide is a valuable approach to promote osteogenic activity at the genetic level. Of interest, MIR31HG plays an essential role in the osteogenic differentiation of MSCs. MIR31HG directly binds to $\text{I}\kappa\text{B}\alpha$ and participates in NF- κB activation.¹⁵ Activated NF- κB promotes β -catenin degradation and inhibits bone formation.²⁶ Additionally, MIR31HG modifies the histone acetylation and methylation in chromatin and subsequently regulates gene expression.²⁴ We fabricated siMIR31HG-functionalized Ti implants and excitingly found that CS/siMIR31HG Ti implants gave rise to significantly enhanced osteogenic activity. The release of siMIR31HG from the biofunctionalized Ti implants may promote osteogenesis of BMSCs via diverse mechanism, including inhibition of NF- κB activation and histone modification.

Clinical application of siRNA therapeutics using drug-loaded delivery systems has been extensively studied. It may serve as a promising technique to treat various diseases.^{27–29} Chitosan is feasible for local delivery of siRNAs,^{30,31} and previous studies have applied chitosan as an oligonucleotide vector in tissue engineering.^{21,22} Recently, chitosan has been used as loading candidate for miRNA^{8,11} and siRNA¹⁹ on a Ti surface and showed excellent delivery efficiency. Our data are consistent with these studies, efficient siRNA release and gene knockdown effect was detected on the siMIR31HG-functionalized Ti implants. Lyophilization has also been reported to store nucleic acid and used to efficiently load nucleic acid complexes onto surfaces.^{32,33} However, the siRNA lyophilization technique has been showed to induce a 30–45% reduction in cell viability.³⁴ Cytocompatibility is a basic requirement for bone implants. In our study, chitosan displayed good biocompatibility. The cells showed comparable viability on all Ti samples and spread well on the CS/siRNA Ti surfaces. The CS/siRNA coating technique demonstrated good safety and high siRNA delivery efficiency.

Before functionalizing the Ti surface with the siRNA complex, the Ti implant needs to be pretreated with thermal alkali to generate a porous structure because the pure Ti surfaces have limited loading capacity. Many procedures are available to increase its reservoir capacity, such as hydrothermal and pressure treatment,³⁵ microarc oxidation treatment.^{36,37} The thermal alkali treatment was applied in this study. This procedure not only generates microporous structure on Ti surface, but also renders the Ti implant negatively charged and ultrahydrophilic, which facilitates physical adsorption of positively charged CS/siRNA particles by electrostatic interactions.^{18–20} As a consequence, it is simple to load the siRNA on the Ti surface by soaking the samples into the CS/siRNA solution.

CONCLUSION

In this study, we loaded siRNA with chitosan vector onto a Ti surface pretreated with thermal alkali. The siMIR31HG-functionalized Ti implant showed an excellent gene knock-down efficiency, and enhanced osteoblastic differentiation of BMSCs in vitro and ectopic bone formation in vivo with no serious cytotoxicity. The siMIR31HG biofunctionalization can be used to achieve better osseointegration of Ti implant in the clinic.

AUTHOR INFORMATION

Corresponding Authors

*E-mail: jialingfei1984@sina.com. Tel.: +86-10-82195778. Fax: +86-10-82193402. Address: Central Laboratory, Peking University School and Hospital of Stomatology, 22 Zhong-guancun South Avenue, Haidian District, Beijing 100081, China (L.J.).

*E-mail: weiranli2003@163.com. Tel.: +86-10-82195332. Fax: +86-10-82195336. Address: Department of Orthodontics, Peking University School and Hospital of Stomatology, 22 Zhongguancun South Avenue, Haidian District, Beijing 100081, China (W.L.).

ORCID

Weiran Li: 0000-0001-9895-1143

Author Contributions

†Y.H. and Y.Z. contributed equally to this work

Notes

The authors declare no competing financial interest.

ACKNOWLEDGMENTS

This study was supported by the National Natural Science Foundation of China (81670957 and 81700938) and Beijing Natural Science Foundation (7172239).

ABBREVIATIONS

RUNX2, runt-related transcription factor 2; OCN, osteocalcin; ALP, alkaline phosphatase; GAPDH, glyceraldehyde 3-phosphate dehydrogenase

REFERENCES

- Franchi, M.; Fini, M.; Martini, D.; Orsini, E.; Leonardi, L.; Ruggeri, A.; Giavaresi, G.; Ottani, V. Biological fixation of endosseous implants. *Micron* **2005**, *36* (7–8), 665–71.
- Liu, X.; Chen, S.; Tsoi, J. K. H.; Matinlinna, J. P. Binary titanium alloys as dental implant materials—a review. *Regen Biomater* **2017**, *4* (5), 315–323.
- Kim, T. I.; Jang, J. H.; Kim, H. W.; Knowles, J. C.; Ku, Y. Biomimetic approach to dental implants. *Curr. Pharm. Des.* **2008**, *14* (22), 2201–11.
- Khan, M. R.; Donos, N.; Salih, V.; Brett, P. M. The enhanced modulation of key bone matrix components by modified Titanium implant surfaces. *Bone* **2012**, *50* (1), 1–8.
- Yang, D. H.; Moon, S. W.; Lee, D. W. Surface Modification of Titanium with BMP-2/GDF-5 by a Heparin Linker and Its Efficacy as a Dental Implant. *Int. J. Mol. Sci.* **2017**, *18* (1), 229.
- Heller, M.; Kumar, V. V.; Pabst, A.; Brieger, J.; Al-Nawas, B.; Kammerer, P. W. Osseous response on linear and cyclic RGD-peptides immobilized on titanium surfaces in vitro and in vivo. *J. Biomed. Mater. Res., Part A* **2018**, *106*, 419.
- Mattick, J. S. RNA regulation: a new genetics? *Nat. Rev. Genet.* **2004**, *5* (4), 316–23.
- Wang, Z.; Wu, G.; Feng, Z.; Bai, S.; Dong, Y.; Wu, G.; Zhao, Y. Microarc-oxidized titanium surfaces functionalized with microRNA-

21-loaded chitosan/hyaluronic acid nanoparticles promote the osteogenic differentiation of human bone marrow mesenchymal stem cells. *Int. J. Nanomed.* **2015**, *10*, 6675–87.

(9) Zhang, X.; Li, Y.; Chen, Y. E.; Chen, J.; Ma, P. X. Cell-free 3D scaffold with two-stage delivery of miRNA-26a to regenerate critical-sized bone defects. *Nat. Commun.* **2016**, *7*, 10376.

(10) Wu, K.; Song, W.; Zhao, L.; Liu, M.; Yan, J.; Andersen, M. O.; Kjems, J.; Gao, S.; Zhang, Y. MicroRNA functionalized microporous titanium oxide surface by lyophilization with enhanced osteogenic activity. *ACS Appl. Mater. Interfaces* **2013**, *5* (7), 2733–44.

(11) Song, W.; Wu, K.; Yan, J.; Zhang, Y.; Zhao, L. MiR-148b laden titanium implant promoting osteogenic differentiation of rat bone marrow mesenchymal stem cells. *RSC Adv.* **2013**, *3* (28), 11292.

(12) Huang, G.; Kang, Y.; Huang, Z.; Zhang, Z.; Meng, F.; Chen, W.; Fu, M.; Liao, W.; Zhang, Z. Identification and Characterization of Long Non-Coding RNAs in Osteogenic Differentiation of Human Adipose-Derived Stem Cells. *Cell. Physiol. Biochem.* **2017**, *42* (3), 1037–1050.

(13) Huynh, N. P.; Anderson, B. A.; Guilak, F.; McAlinden, A. Emerging roles for long noncoding RNAs in skeletal biology and disease. *Connect. Tissue Res.* **2017**, *58* (1), 116–141.

(14) Montes, M.; Nielsen, M. M.; Maglieri, G.; Jacobsen, A.; Hofjeldt, J.; Agrawal-Singh, S.; Hansen, K.; Helin, K.; van de Werken, H. J.; Pedersen, J. S.; Lund, A. H. The lncRNA MIR31HG regulates p16(INK4A) expression to modulate senescence. *Nat. Commun.* **2015**, *6*, 6967.

(15) Jin, C.; Jia, L.; Huang, Y.; Zheng, Y.; Du, N.; Liu, Y.; Zhou, Y. Inhibition of lncRNA MIR31HG Promotes Osteogenic Differentiation of Human Adipose-Derived Stem Cells. *Stem Cells* **2016**, *34* (11), 2707–2720.

(16) Monaghan, M.; Pandit, A. RNA interference therapy via functionalized scaffolds. *Adv. Drug Delivery Rev.* **2011**, *63* (4–5), 197–208.

(17) Saito, T.; Tabata, Y. Preparation of gelatin hydrogels incorporating small interfering RNA for the controlled release. *J. Drug Target* **2012**, *20* (10), 864–72.

(18) Nishiguchi, S.; Kato, H.; Fujita, H.; Oka, M.; Kim, H. M.; Kokubo, T.; Nakamura, T. Titanium metals form direct bonding to bone after alkali and heat treatments. *Biomaterials* **2001**, *22* (18), 2525–33.

(19) Zhang, L.; Wu, K.; Song, W.; Xu, H.; An, R.; Zhao, L.; Liu, B.; Zhang, Y. Chitosan/siCkip-1 biofunctionalized titanium implant for improved osseointegration in the osteoporotic condition. *Sci. Rep.* **2015**, *5*, 10860.

(20) Hu, X.; Neoh, K. G.; Zhang, J.; Kang, E. T. Bacterial and osteoblast behavior on titanium, cobalt-chromium alloy and stainless steel treated with alkali and heat: a comparative study for potential orthopedic applications. *J. Colloid Interface Sci.* **2014**, *417*, 410–9.

(21) Liu, X.; Howard, K. A.; Dong, M.; Andersen, M. O.; Rahbek, U. L.; Johnsen, M. G.; Hansen, O. C.; Besenbacher, F.; Kjems, J. The influence of polymeric properties on chitosan/siRNA nanoparticle formulation and gene silencing. *Biomaterials* **2007**, *28* (6), 1280–8.

(22) Rudzinski, W. E.; Aminabhavi, T. M. Chitosan as a carrier for targeted delivery of small interfering RNA. *Int. J. Pharm.* **2010**, *399* (1–2), 1–11.

(23) Song, W.; Yang, C.; Svend Le, D. Q.; Zhang, Y.; Kjems, J. Calcium-MicroRNA Complex-Functionalized Nanotubular Implant Surface for Highly Efficient Transfection and Enhanced Osteogenesis of Mesenchymal Stem Cells. *ACS Appl. Mater. Interfaces* **2018**, *10* (9), 7756–7764.

(24) Huang, Y.; Jin, C.; Zheng, Y.; Li, X.; Zhang, S.; Zhang, Y.; Jia, L.; Li, W. Knockdown of lncRNA MIR31HG inhibits adipocyte differentiation of human adipose-derived stem cells via histone modification of FABP4. *Sci. Rep.* **2017**, *7* (1), 8080.

(25) Huang, Y.; Zheng, Y.; Jia, L.; Li, W. Long Noncoding RNA H19 Promotes Osteoblast Differentiation Via TGF-beta1/Smad3/HDAC Signaling Pathway by Deriving miR-675. *Stem Cells* **2015**, *33* (12), 3481–92.

(26) Chang, J.; Liu, F.; Lee, M.; Wu, B.; Ting, K.; Zara, J. N.; Soo, C.; Al Hezaimi, K.; Zou, W.; Chen, X.; Mooney, D. J.; Wang, C. Y. NF-kappaB inhibits osteogenic differentiation of mesenchymal stem cells by promoting beta-catenin degradation. *Proc. Natl. Acad. Sci. U. S. A.* **2013**, *110* (23), 9469–74.

(27) Bang, E. K.; Cho, H.; Jeon, S. S.; Tran, N. L.; Lim, D. K.; Hur, W.; Sim, T. Amphiphilic small peptides for delivery of plasmid DNAs and siRNAs. *Chem. Biol. Drug Des.* **2018**, *91*, 575.

(28) Dunn, S. S.; Tian, S.; Blake, S.; Wang, J.; Galloway, A. L.; Murphy, A.; Pohlhaus, P. D.; Rolland, J. P.; Napier, M. E.; DeSimone, J. M. Reductively responsive siRNA-conjugated hydrogel nanoparticles for gene silencing. *J. Am. Chem. Soc.* **2012**, *134* (17), 7423–30.

(29) Li, Y. L.; Quarles, L. D.; Zhou, H. H.; Xiao, Z. S. RNA interference and its application in bone-related diseases. *Biochem. Biophys. Res. Commun.* **2007**, *361* (4), 817–21.

(30) Buschmann, M. D.; Merzouki, A.; Lavertu, M.; Thibault, M.; Jean, M.; Darras, V. Chitosans for delivery of nucleic acids. *Adv. Drug Delivery Rev.* **2013**, *65* (9), 1234–70.

(31) Tezgel, O.; Szarpak-Jankowska, A.; Arnould, A.; Auzely-Velty, R.; Texier, I. Chitosan-lipid nanoparticles (CS-LNPs): Application to siRNA delivery. *J. Colloid Interface Sci.* **2018**, *510*, 45–56.

(32) Ball, R. L.; Bajaj, P.; Whitehead, K. A. Achieving long-term stability of lipid nanoparticles: examining the effect of pH, temperature, and lyophilization. *Int. J. Nanomed.* **2017**, *12*, 305–315.

(33) Kasper, J. C.; Troiber, C.; Kuchler, S.; Wagner, E.; Friess, W. Formulation development of lyophilized, long-term stable siRNA/oligoaminoamide polyplexes. *Eur. J. Pharm. Biopharm.* **2013**, *85* (2), 294–305.

(34) Andersen, M. O.; Nygaard, J. V.; Burns, J. S.; Raarup, M. K.; Nyengaard, J. R.; Bunker, C.; Besenbacher, F.; Howard, K. A.; Kassem, M.; Kjems, J. siRNA nanoparticle functionalization of nanostructured scaffolds enables controlled multilineage differentiation of stem cells. *Mol. Ther.* **2010**, *18* (11), 2018–27.

(35) Guo, Z.; Jiang, N.; Chen, C.; Zhu, S.; Zhang, L.; Li, Y. Surface bioactivation through the nanostructured layer on titanium modified by facile HPT treatment. *Sci. Rep.* **2017**, *7* (1), 4155.

(36) Bai, Y.; Zhou, R.; Cao, J.; Wei, D.; Du, Q.; Li, B.; Wang, Y.; Jia, D.; Zhou, Y. Microarc oxidation coating covered Ti implants with micro-scale gouges formed by a multi-step treatment for improving osseointegration. *Mater. Sci. Eng., C* **2017**, *76*, 908–917.

(37) Zhou, R.; Wei, D.; Cao, J.; Feng, W.; Cheng, S.; Du, Q.; Li, B.; Wang, Y.; Jia, D.; Zhou, Y. Synergistic effects of surface chemistry and topologic structure from modified microarc oxidation coatings on Ti implants for improving osseointegration. *ACS Appl. Mater. Interfaces* **2015**, *7* (16), 8932–41.